AIChE

Experimental Investigation on Evaporation of Urea-Water-Solution Droplet for SCR Applications

Tae Joong Wang, Seung Wook Baek, and Seung Yeol Lee
Propulsion and Combustion Laboratory, School of Mechanical, Aerospace and Systems Engineering, Korea Advanced Institute of Science and Technology (KAIST), 373-1 Guseong-dong, Yuseong-gu, Daejeon 305-701, Republic of Korea

Dae Hwan Kang
Head of Technology Center, Technology Center, ORDEG Corporation, 404 Mognae-dong, Danwon-gu, Ansan-si, Gyeonggi-do 425-100, Republic of Korea

Gwon Koo Yeo
Principal Research Engineer, Emission Research Team, Advanced Technology Center, Hyundai-Kia Motors, 772-1 Jangduk-dong, Hwaseong-si, Gyeonggi-do 445-706, Republic of Korea

DOI 10.1002/aic.11939
Published online August 13, 2009 in Wiley InterScience (www.interscience.wiley.com).

The evaporation behavior of urea-water-solution (UWS) droplet was investigated for application to urea-selective catalytic reduction (SCR) systems. A number of experiments were performed with single UWS droplet suspended on the tip of a fine quartz fiber. To cover the temperature range of real-world diesel exhausts, droplet ambient temperature was regulated from 373 to 873 K using an electrical furnace. As a result of this study, UWS droplet revealed different evaporation characteristics depending on its ambient temperature. At high temperatures, it showed quite complicated behaviors such as bubble formation, distortion, and partial rupture after a linear D^2-law period. However, as temperature decreases, these phenomena became weak and finally disappeared. Also, droplet diminishment coefficients were extracted from transient evaporation histories for various ambient temperatures, which yields a quantitative evaluation on evaporation characteristics of UWS droplet as well as provides valuable empirical data required for modeling or simulation works on urea-SCR systems. © 2009 American Institute of Chemical Engineers *AIChE J,* 55: 3267–3276, 2009
Keywords: evaporation, aqueous solutions, selective catalytic reduction, NO_x, urea

Introduction

Among various techniques of SCR, the most realistic solution capable of reducing diesel NO_x to levels required by stringent worldwide emission standards is ammonia-selective catalytic reduction (SCR) which uses ammonia as a reducing agent.[1] However, due to inherent toxicity and handling problems with pure ammonia, aqueous urea solution is now practically utilized as an alternative to the direct use of ammonia for mobile SCR applications.

Once urea-water-solution (UWS) spray is injected into hot exhaust gas stream before SCR catalyst, water content first

Correspondence concerning this article should be addressed to T. J. Wang at cakecandle@kaist.ac.kr

evaporates from UWS. Then, ammonia is generated in-situ through both thermal decomposition of urea and hydrolysis of isocyanic acid as follows.[2–4]

$$(NH_2)_2CO \rightarrow NH_3 + HNCO \quad (1)$$

$$HNCO + H_2O \rightarrow NH_3 + CO_2 \quad (2)$$

By collectively reviewing the literatures,[5–8] it is found that the state of aggregation urea is not clear during the evaporation of UWS, rather it can be varied among solid, molten, and gas phases depending on thermo-physical conditions.

After that, ammonia produced by the above reactions 1 and 2 takes part in various deNO_x reactions as a reductant. Main deNO_x reactions under a typical diesel exhaust environment can be summarized as follows.[5,9]

$$4NH_3 + 4NO + O_2 \rightarrow 4N_2 + 6H_2O \quad (3)$$

$$4NH_3 + 2NO + 2NO_2 \rightarrow 4N_2 + 6H_2O \quad (4)$$

$$4NH_3 + 3NO_2 \rightarrow 7/2N_2 + 6H_2O \quad (5)$$

$$4NH_3 + 4NO + 3O_2 \rightarrow 4N_2O + 6H_2O \quad (6)$$

In addition to the removal of NO_x with ammonia, a direct reduction of NO by urea and isocyanic acid is also reported such that[8,10]

$$2(NH_2)_2CO + 6NO \rightarrow 5N_2 + 4H_2O + 2CO_2 \quad (7)$$

$$4HNCO + 6NO \rightarrow 5N_2 + 2H_2O + 4CO_2 \quad (8)$$

Fang and DaCosta,[8] on the basis of engine test results, suggested that so-called standard and fast SCR reactions (i.e., reactions 3 and 4, respectively) may not be major routes in NO_x abatement, whereas reactions 7 and 8 may play an important role in SCR processes.

However, in urea-SCR systems, several negative effects are possibly derived due to the use of UWS. Sullivan and Doherty,[11] on the basis of experiments with several oxide-supported copper catalysts, proposed a possibility that urea does not hydrolyze according to reactions 1 and 2 and instead it reacts with O_2 to form N_2 fruitlessly as follows.

$$(NH_2)_2CO + O_2 \rightarrow CO_2 + H_2O + N_2 \quad (9)$$

Moreover, deposit formation is a highly critical problem. Various urea decomposition products (i.e., biuret, cyanuric acid (CYA), ammelide, ammeline, melamine, etc.) and their polymeric complexes involving hydrogen bondings can be generated in urea-SCR systems. Fang and DaCosta[8] reported that urea thermolysis involves two decomposition stages; one is ammonia generation stage which is desirable for reducing NO_x, whereas the other is ammonia consumption stage which promotes the formation of undesirable species. In particular, consecutive decompositions after ammonia consumption stage lead to the production of melamine complexes, $(HNC{=}NH)_x(HNCO)_y$, which are considered as a major source to hinder the performance of catalyst by not only consuming a part of ammonia produced during urea thermolysis but also degrading the structural and thermal properties of catalyst surface.

A sufficient understanding on the behavior of UWS spray is prerequisite for controlling the formation of urea-derived deposits. However, there are lots of complexities involved in the evaporation process of UWS at a heated environment. Dissolved urea influences the evaporation of water from UWS and simultaneously urea itself undergoes thermal decomposition as well as reacts to produce various species. Because of these difficulties, the evaporation behavior of UWS has not been clearly understood yet.

Recently, Birkhold et al.[12] numerically investigated the evaporation of UWS droplet by using several models, and therein the rapid mixing model was selected as the best one while considering a trade-off between cost and accuracy. In the rapid mixing model, infinitely fast transport is assumed for liquid phase which results in spatially uniform temperature, concentration, and fluid properties of droplet, but these quantities change in time.[13–14]

In this study, the evaporation behavior of UWS droplet was experimentally observed over the temperature range of actual diesel exhaust. Measurements were conducted by changing droplet ambient temperature by 50 K from 373 to 873 K. Main objectives of this study are to understand the evaporation characteristics of UWS droplet in various ambient temperatures and also to provide empirical evaporation coefficients which can be utilized as reference data in modeling or simulation works on UWS spray. So far, to our knowledge, there have been few useful experimental data capable of quantifying the evaporation of UWS droplet over a wide range of temperatures.

As typically appeared in the evaporation process of multicomponent fuel droplet or emulsified mixture droplet, the phenomenon of violent droplet fragmentation which is often referred to as microexplosion is also observed during the evaporation of UWS droplets at elevated temperatures in this study. The basic mechanism responsible for microexplosion can be best explained through the diffusion limit model.[15–18] More volatile component trapped in droplet interior due to diffusional resistance can be heated beyond local boiling point and hence undergoes internal superheating. This may eventually lead to the onset of homogeneous nucleation, whose extremely rapid rate of gasification causes intense internal pressure build-up and thereby disruptive droplet fragmentation. Law[15] suggested that microexplosion is a possible mechanism to prevent the formation of large coal particle agglomerates in evaporating coal slurry droplets. In this study, it was explored how microexplosion affects both the evaporation of UWS droplet and the formation of urea-derived deposits under a variety of ambient temperatures.

In this experiment, observations were conducted for the UWS droplets evaporating at stagnant state. However, in actual spray systems, droplet internal circulation is induced by the inertia acquired during its injection. A relative motion between droplet and ambient gas results in shear at interface, which leads the liquid near droplet surface to recirculate internally.[14] Although this recirculation enhances the internal mixing of an injected multicomponent droplet, the occurrence of microexplosion is also justified. Lara-Urbaneja and Sirignano[19] reported that the disruptive behaviors of droplet

can be observed even at high Reynolds number because part of light component remains inside multicomponent droplet until the end of its lifetime. Hence, despite a fast diffusion is able to prevent microexplosion by allowing light component to easily leave droplet, internal circulation will not avoid it. This strongly supports the view that microexplosion phenomena observed in the current type of stationary droplet experiment also characterize the evaporation process of sprayed droplets. Note that the droplet evaporation rate in forced convection environment can be quantitatively predicted with a stagnant rate using such empirical correlations as summarized in Chiu.[20]

The initial diameter of UWS droplets used in this experiment ranges from about 700–1450 μm. Note that 700 μm is the lowest limit of the present experimental facility which uses suspended droplets. Regarding that the initial Sauter mean diameter (SMD) of UWS spray applied in practical systems ranges from about 20–150 μm,[12] it is found that there exists quite a big (almost 10 times) difference in initial droplet size between the current experiment and its application. According to the D^2-law of droplet (for a review, see Ref. 21), the evaporation coefficient of liquid droplet is independent of its initial diameter. However, this is not applicable directly to the current case because the evaporation process of multicomponent droplet is inherently transient due to temporal variations in its temperature and composition.[22] Therefore in this study, for an extension of the results to much smaller-size droplets, the effect of initial droplet size on its evaporation was investigated through a number of experiments under a variety of initial diameters and ambient temperatures.

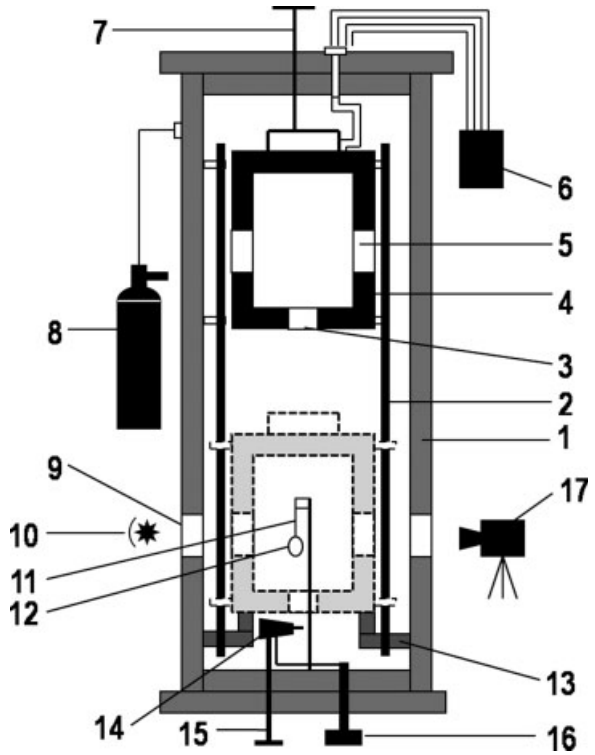

Figure 1. A schematic view of experimental setup.

1: cylindrical vessel, 2: guide bar, 3: furnace bottom hole, 4: electric furnace, 5: quartz glass window on furnace, 6: temperature controller, 7: furnace lever, 8: air vessel, 9: quartz glass window on pressure vessel, 10: backlight source, 11: quartz fiber, 12: droplet, 13: shock absorber, 14: droplet maker, 15: droplet lever, 16: plunger micro-pump, 17: high-speed CCD camera.

Experiments

Procedures and facilities

In this study, AdBlue (contains 32.5% urea by weight) is used as a representative UWS. A schematic view of experimental setup is illustrated in Figure 1. In this section, experimental procedures and facilities are described and further details can be found in Ghassemi et al.[23,24]

First, an electrical furnace is lifted up away from a droplet suspension system and its interior temperature is regulated to an intended value using controller and thermocouple. At the same time, a cylindrical vessel (height = 0.8 m, inner diameter = 0.15 m) is purged by a pressurized dry air at room temperature, which refreshes the ambience of droplet. Actually, exhaust gases from diesel engines typically contain a significant amount of water (~5–10%) and this water content may influence the thermal decomposition process of urea.[8] Nevertheless, the current experimental results obtained at dry ambient condition can possibly act as a reference to those of humid environment.

Once the control of droplet ambient temperature is completed, then single UWS droplet is suspended around a bead that is placed at the tip of a quartz fiber (diameter = 0.125 mm) using a droplet maker whose end part is equipped with a hollow stainless-steel needle (outer diameter = 0.21 mm). The movement of this droplet maker is adjusted by handling a lever, which causes liquid UWS to transport to the bead, thereby generating a droplet.

For continuous monitoring of droplet ambient temperature, a K-type thermocouple was placed about 30 mm beside suspended droplet. In this experiment, solidified deposit was finally remained around bead over a wide range of temperatures so that a small torch flame was used to completely remove it for next measurement. However, repetitive exposures of thin quartz fiber to elevated temperatures made it brittle and therefore the fiber was replaced by new one after several tens of measurements. Note that, because the bead was made by melting the end part of quartz fiber using a high-temperature torch flame, the diameter of each bead was not a constant, rather it varied from about 0.25–0.3 mm.

The next step is to drop electrical furnace to the position as shown in dotted line in Figure 1. Then, this leads the suspended UWS droplet to be exposed to high temperature, which eventually yields its evaporation. Glass window enables us to observe the evaporation process of droplet using a high-speed charge-coupled device (CCD) camera and its pictured images are recorded on a computer. Post-processing procedures to get quantitative data from these sequential pictures are explained in the next section.

It should be noted that there are several error sources in measuring the evaporation rate of UWS droplet under a constant temperature condition. Despite these errors, a certain degree of measurement accuracy may be conserved in this study. By virtue of self-controlling temperature system as well

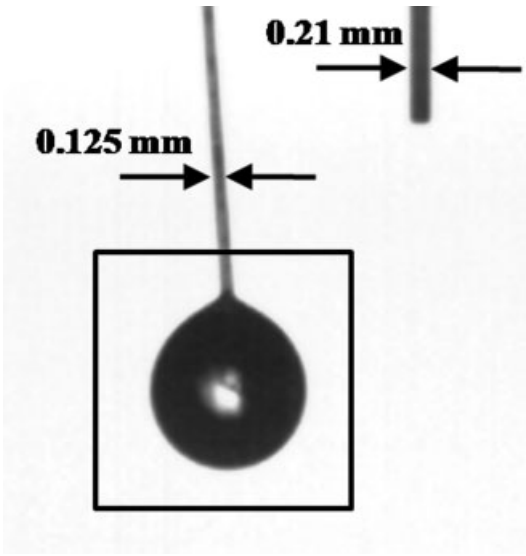

Figure 2. A sample photograph of evaporating UWS droplet (droplet diameter: 1.289 mm).

as rapid increase in temperature using electrical heating element, it is possible to sustain the ambient temperature of droplet to a nearly constant value without significant variation. In addition, conduction heat transfer between fiber and droplet is almost negligible because the thickness of quartz suspension fiber is very thin. Radiation heat transfer from heating element coils placed at furnace inner walls to droplet is also minimized using radiative shields equipped around the coils.

However, an amount of fresh air at room temperature inevitably flows into high-temperature furnace during its fall. As a result, furnace inner temperature fluctuates a little while UWS droplet is evaporated, especially in early evaporation period. Note that this fluctuation bandwidth becomes wider as the initial temperature of furnace increases due to a larger temperature difference between furnace inside and fresh air.

Extracting droplet diameter and evaporation coefficient

Figure 2 shows a sample of image of UWS droplet that was captured during evaporation. Here, the needle beside droplet-suspended fiber provides a reference scale of known diameter (0.21 mm). To extract droplet diameter from the picture, a flexible image-processing program was developed using Visual Basic language. In this program, the number of pixels corresponding to the diameter of reference needle is first calculated. Then, an imaginary square of known area is drawn around droplet as shown in Figure 2. After that, the number of pixels that constitute droplet is calculated on the basis of intensity difference from surroundings. Finally, the area of a concentric circle having the same number of pixels is calculated, which in turns gives droplet diameter from the law of proportion with reference needle. This procedure is executed iteratively for each image file, which yields a temporal variation of droplet diameter during evaporation. Note that the shape of suspended droplet is not an exactly concentric circle due to both gravitation and droplet-fiber interaction. This eccentricity becomes severe as initial droplet size decreases, which may lead to some measurement errors.

In general, the early lifetime of evaporating droplet shows a nonlinear behavior due to transient droplet heat-up from environment and subsequent thermal expansion. As droplet temperature increases, a balance between thermal expansion and evaporation determines the size of droplet at that time. Once the temperature inside droplet reaches a quasi-steady state, only evaporation becomes effective in determination of the size of droplet. Starting from this stage, an evaporation process according to the D^2-law of droplet becomes valid. In droplet evaporation studies, initial heat-up period does not have any importance because evaporation rate is generally evaluated by its subsequent period. Moreover, as initial droplet size becomes smaller, this initial heat-up period becomes negligible.[23] Regarding the linear D^2-law part, droplet evaporation is quantitatively characterized by the following evaporation coefficient, K.

$$K = \frac{d(D^2)}{dt} \tag{10}$$

This droplet evaporation coefficient is extracted from the temporal history of squared droplet diameter by measuring the slope of its linear regression part. In this study, the above procedure is also used to obtain the evaporation coefficient of UWS droplet.

Results and Discussion

Evaporation characteristics of UWS droplet with ambient temperature

Figure 3 shows normalized temporal variations of the diameter squared of UWS droplets evaporating at ambient

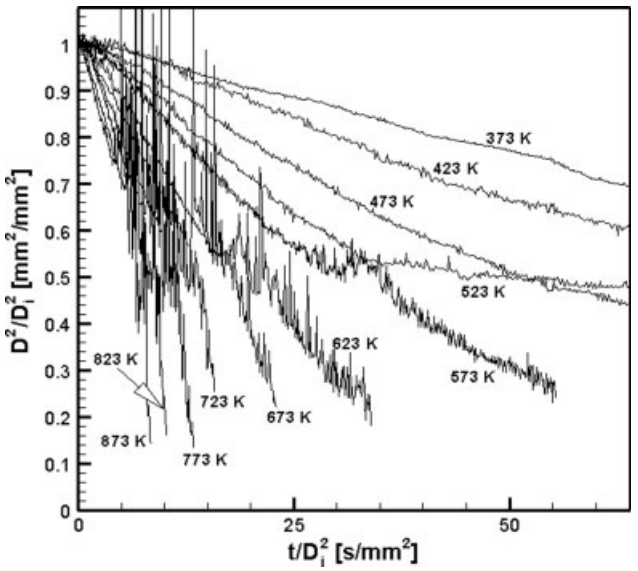

Figure 3. Normalized temporal variations of the diameter squared of evaporating UWS droplets with ambient temperature.

Initial droplet diameter: 0.963 mm at 373 K, 0.758 mm at 423 K, 0.870 mm at 473 K, 0.857 mm at 523 K, 0.920 mm at 573 K, 0.869 mm at 623 K, 0.815 mm at 673 K, 0.761 mm at 723 K, 0.905 mm at 773 K, 0.874 mm at 823 K, 0.816 mm at 873 K.

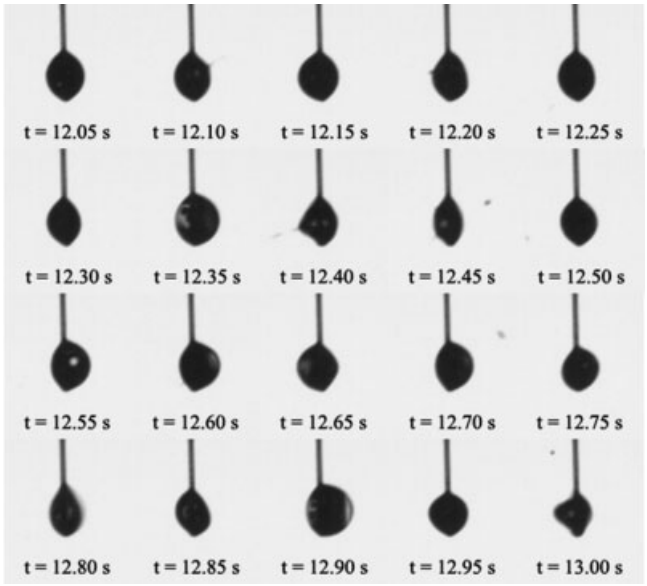

Figure 4. Sequential photographs of evaporating UWS droplet at 773 K which show microexplosion.

Initial droplet diameter: 1.131 mm, camera speed: 20 fps.

temperatures from 373 to 873 K. Note that, to minimize initial droplet size effect on its evaporation, experiments were performed with the droplets having similar initial diameters (from 0.758 to 0.963 mm). As clearly shown in the figure, UWS droplets displayed different evaporation behaviors depending on their ambient temperature. From this observation, the evaporation characteristics of UWS droplet can be classified into several groups according to the range of ambient temperature.

Also, Figure 3 reveals that droplet microexplosion begins to appear at 573 K and it becomes more intense with increase in ambient temperature. Figure 4 presents sequential photographs of evaporating UWS droplet at 773 K and microexplosion phenomenon is clearly observed here. Droplet internal bubble formation appears from the photos pictured at 12.35, 12.55, 12.60, 12.65, and 12.90 s because of its rapid expansion. Also, droplet distortion is seen from the photos of 12.20, 12.40, 12.85, and 13.00 s and droplet fragmentation is shown from the photos of 12.10, 12.20, 12.40, 12.45, 12.70, and 13.00 s. Note that these irregular behaviors are typically observed in the evaporation process of multicomponent droplet.[23]

For ambient temperatures of 373 and 423 K

As shown in Figure 3, UWS droplets evaporating at both 373 and 423 K exhibit almost linear history. For more detailed analysis, the whole lifetime of each droplet is presented in Figure 5. Here, the evaporation history of each droplet is displayed up to 0.617 mm^2/mm^2 for 373 K and up to 0.522 mm^2/mm^2 for 423 K. This is because liquid component constituting UWS droplets is completely evaporated at these points and hereafter almost no more reduction in droplet overall size is observed.

The melting point of urea is known to 406 $\pm$ 3 K.[25] Therefore, at ambient temperature of 373 K, only water content will evaporate from UWS droplet. On the other hand, at 423 K, urea near droplet surface is expected to melt and thermally decomposes into ammonia and isocyanic acid according to reaction 1. However, as shown in Figure 5, the current experimental result at 423 K exhibits a similar evaporation behavior to that of 373 K. Hence, urea gasification was not clearly observed at 423 K in this study. This observation is consistent with the result produced by Schaber et al.[7] who reported that a vigorous gas evolution from molten urea commences at 425 K.

To estimate the evaporation coefficient of UWS droplet, the least square regression method was used with the data corresponding to linear part of evaporation history except both initial heat-up and final solidification periods. The estimated evaporation coefficients were given with actual measurement data in Figure 5.

It is worthwhile to note that solidified deposit remains after the complete depletion of liquid component from UWS droplets at both 373 and 423 K. The deposits produced at these ambient temperatures may be composed only of solidified urea because the first urea-derived species, biuret, begins to be generated from the reaction of isocyanic acid with intact urea at $\sim$433 K.[7] Sequential photographs including evaporation and solidification processes of UWS droplet at 373 K are displayed in Figure 6, and therein observations after 75 s indicate that deposit undergoes no change until the end of camera capture. At 373 K, UWS droplet shows solid-like behavior because dissolved urea is never melted at this ambient temperature during the whole evaporation period.

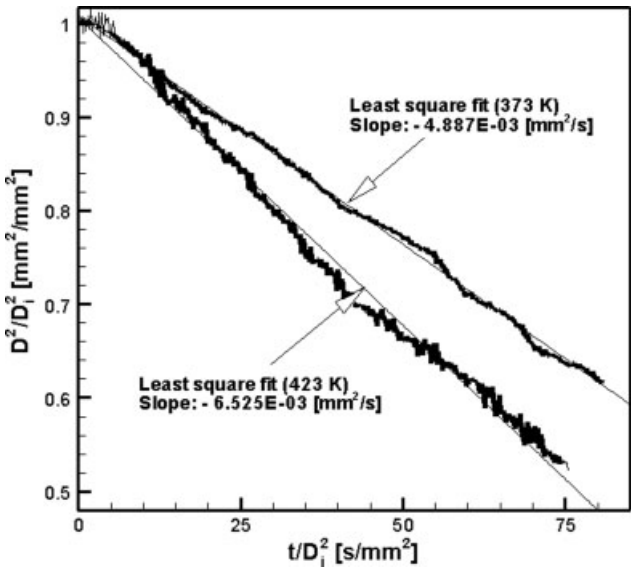

Figure 5. Normalized temporal variations of the diameter squared of evaporating UWS droplets with the least square fit to linear water evaporation part (bold solid fine) at both 373 K and 423 K.

For 373 K, initial droplet diameter: 0.963 mm, camera speed: 10 fps, ambient temperatures measured during evaporation: 372 - 374 K. For 423 K, initial droplet diameter: 0.758 mm, camera speed: 10 fps, ambient temperatures measured during evaporation: 423 - 427 K.

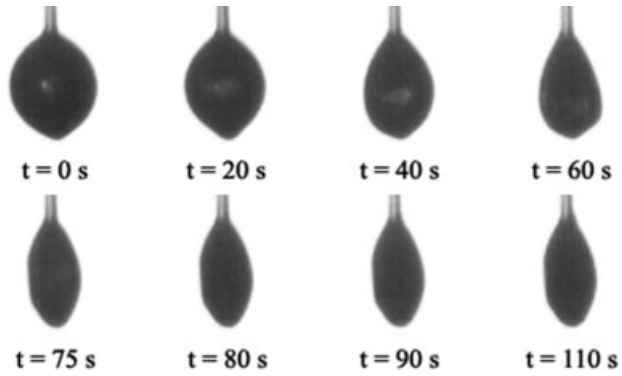

Figure 6. Sequential photographs of evaporating UWS droplet at 373 K.

Initial droplet diameter: 0.963 mm, camera speed: 10 fps.

On the other hand, at 423 K, UWS droplet exhibits more liquid-like characteristic during evaporation because dissolved urea is possibly heated over its melting point and, therefore, exists as a molten state at this temperature.

For ambient temperatures of 473 and 523 K

Figure 7 displays normalized temporal variations of the diameter squared of evaporating UWS droplets at both 473 and 523 K. As shown in the figure, evaporation histories at these ambient temperatures can be divided into two distinguished stages because of the obvious difference in their diminishing rates. For 473 K, the first stage is up to 51 s/mm^2, while the second stage is from 51 to 250 s/mm^2. Also, for 523 K, the first stage is up to 33 s/mm^2, while the second stage is from 33 to 129 s/mm^2. During the first-stage evaporation period, it is expected that water content mainly evaporates from UWS droplets. Musa et al.[26] compared the evaporation behavior of UWS droplet with distilled water and therein almost no difference in their first-stage evaporation was observed. On the other hand, during the second-stage evaporation, the gasification of urea may be a dominant mechanism responsible for diminishment in UWS droplet size. Note that this two-stage type of evaporation characteristics observed at these ambient temperatures support the employment of the rapid mixing model for estimating evaporation rate of UWS droplet as in Birkhold et al.[12]

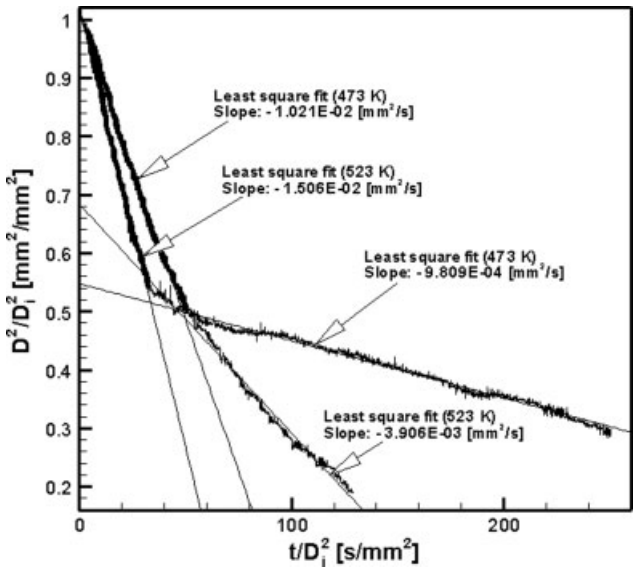

Figure 7. Normalized temporal variations of the diameter squared of evaporating UWS droplets with the least square fits to linear water evaporation part (bold solid line) and to linear urea gasification part (thin solid line) at both 473 K and 523 K.

For 473 K, initial droplet diameter: 0.870 mm, camera speed; 10 fps, ambient temperatures measured during evaporation: 469 - 475 K. For 523 K, initial droplet diameter: 0.857 mm, camera speed: 10 fps, ambient temperatures measured during evaporation: 519 - 527 K.

Previously, at temperatures of 373 and 423 K, urea gasification did not appear to occur. However, at 473 and 523 K, it was clearly observed after the complete depletion of liquid component. Perhaps, this is because the decomposition of urea rapidly enhances above 425 K.[7] Therefore, at temperatures of 473 and 523 K, the diminishment rate of UWS droplet should be determined respectively for both stages to completely quantify its entire evaporation period. Here, the least square method was also utilized to find the slope of each stage. A comparison of two evaporation histories presented in Figure 7 indicates that the difference in the slope of each stage becomes smaller with increase in ambient temperature. Figure 8 displays sequential photographs of evaporating UWS droplet at 473 K and there is almost no difference in apparent evaporation behavior for each stage except the magnitude of diminishment rate.

Also, at these temperatures, solidified deposit was observed to remain finally as in the previous case of 373 and 423 K. However, its constituents may be different. Referring to the pyrolysis experiment conducted by Schaber et al.,[7] the deposits generated at 473 and 523 K probably consist of several urea-derived products such as biuret, CYA, ammelide, and ammiline with the undecomposed urea itself.

For ambient temperatures of 573 and 623 K

Figure 9 shows normalized evaporation histories at both 573 and 623 K. The most distinguished feature of

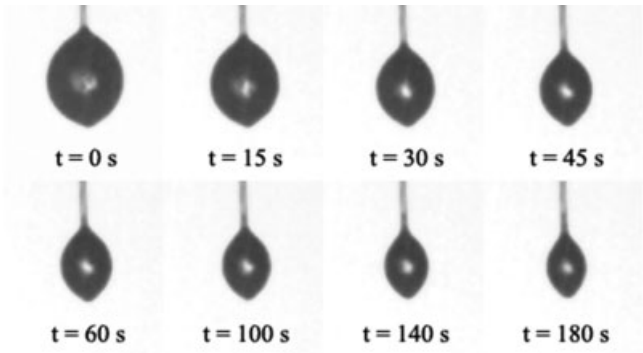

Figure 8. Sequential photographs of evaporating UWS droplet at 473 K.

Initial droplet diameter: 0.870 mm, camera speed: 10 fps.

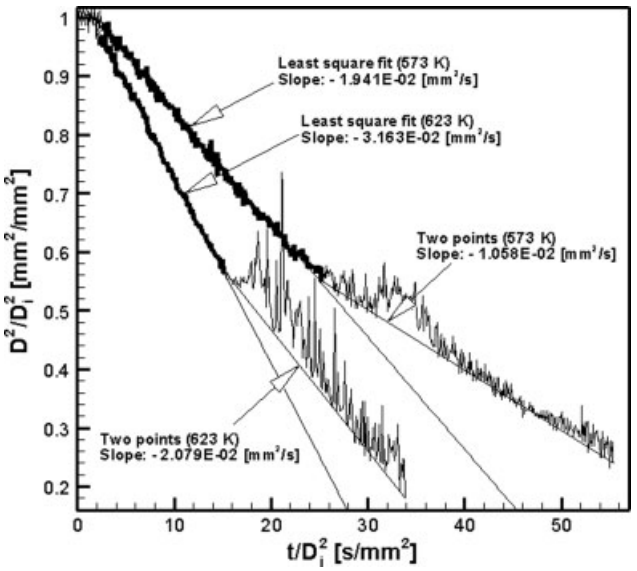

Figure 9. Normalized temporal variations of the diameter squared of evaporating UWS droplets with the least square fit to linear water evaporation part (bold solid line) and two-point estimation to urea gasification part (thin solid line) at both 573 K and 623 K.

For 573 K, initial droplet diameter: 0.920 mm, camera speed: 15 fps, ambient temperatures measured during evaporation: 567 - 575 K. For 623 K, initial droplet diameter: 0.869 mm, camera speed: 15 fps, ambient temperatures measured during evaporation: 620 - 627 K.

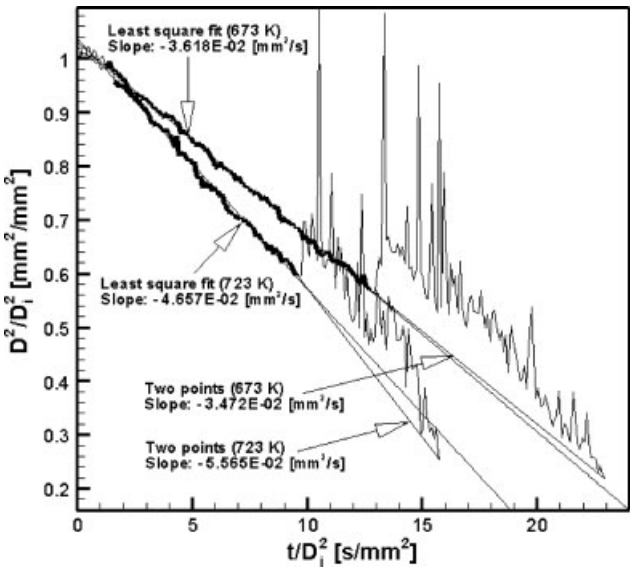

Figure 11. Normalized temporal variations of the diameter squared of evaporating UWS droplets with the least square fit to linear water evaporation part (bold solid line) and two-point estimation to urea gasification part (thin solid line) at both 673 K and 723 K.

For 673 K, initial droplet diameter: 0.815 mm, camera speed: 15 fps, ambient temperatures measured during evaporation: 670 - 677 K. For 723 K, initial droplet diameter: 0.761 mm, camera speed: 20 fps, ambient temperatures measured during evaporation: 723 - 730 K.

evaporating UWS droplets at these ambient temperatures is the onset of microexplosion. In Figure 9, after the first linear evaporation period, droplet re-expansion is observed with a fluctuating behavior. The reason for this fluctuation is that, as mentioned previously, more volatile component trapped inside UWS droplet due to diffusional resistance is heated beyond local boiling point, which causes homogeneous nucleation and thereby droplet internal pressure build-up. Here, the rates of both nucleation and diffusion compete against each other, whose difference influences droplet expansion characteristics. A comparison of two evaporation histories reveals that more intense fluctuation occurs at higher temperature. A fast internal pressure build-up caused by rapid nucleation at higher temperature results in more aggressive evaporation behaviors such as bigger expansion, more severe bubble formation, and more disruptive fragmentation.

To obtain the evaporation coefficient of the first stage, the least square method was also applied to the linear part of experimental data. However, for the next evaporation stage, the use of the least square method is not justified due to droplet expansion and fluctuation so that its diminishment rate is simply estimated using the slope determined with two end points. Note that, from the comparison of two evaporation histories, the difference in diminishment rates of both the first and the second stages becomes smaller as ambient temperature increases.

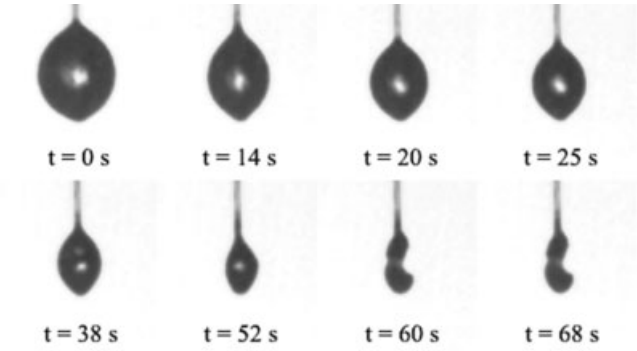

Figure 10. Sequential photographs of evaporating UWS droplet at 573 K.

Initial droplet diameter: 0.870 mm, camera speed: 10 fps.

Figure 12. Photographs of solidified deposits remaining after the complete evaporation of UWS droplets for various ambient temperatures.

Initial droplet diameter: 1.039 mm at 623 K, 1.105 mm at 673 K, 1.067 mm at 723 K, 1.131 mm at 773 K, 1.034 mm at 823 K.

Sequential photographs of the whole evaporation process at 573 K are displayed in Figure 10. At temperatures of 573 and 623 K, solidified deposits were also observed to remain after the complete depletion of liquid component. However, their amount is much smaller when compared with the previous lower-temperature cases. It should be noted that these deposits may be composed of the same constituents as those of 473 and 523 K.

For ambient temperatures of 673 and 723 K

Figure 11 illustrates normalized evaporation histories of UWS droplets at 673 and 723 K. In this experiment, there was almost no difference in evaporation characteristics at ambient temperatures above 673 K. Hence, evaporation histories obtained over 673 K showed the same profile as displayed in Figure 11 except for the magnitude of their slope. The diminishment rates of both the first and the second stages were increased with ambient temperature. Particularly in these temperatures of 673 and 723 K, the magnitude of the first-stage evaporation rate is almost equal to that of the second-stage rate as can be seen from both evaporation histories in Figure 11.

Photographs of solidified deposits remaining after the complete depletion of liquid component at temperatures from 623 to 823 K are displayed in Figure 12. As shown in the pictures, the amount of deposit remained was considerably reduced as ambient temperature rises from 623 to 673 K. This may be attributed that the decomposition of CYA is completed between 648 and 653 K as well as the sublimation and decomposition of ammelide occurs significantly at temperatures from 623 to 673 K.[7]

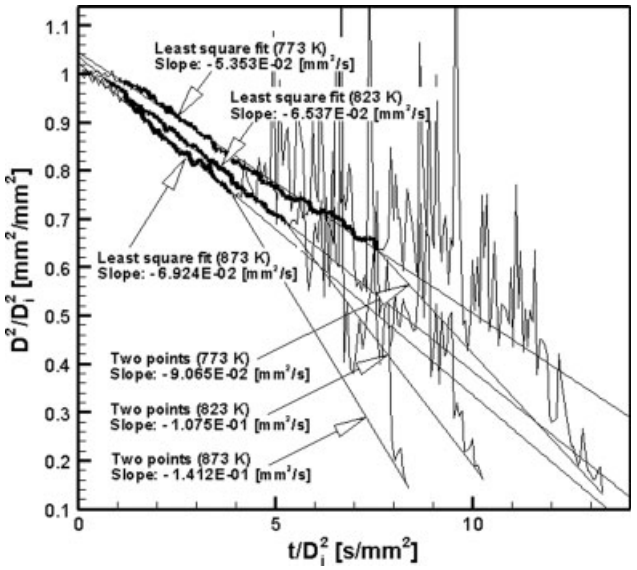

Figure 13. Normalized temporal variations of the diameter squared of evaporating UWS droplets with the least square fit to linear water evaporation part (bold solid line) and two-point estimation to urea gasification part (thin solid line) at 773 K, 823 K, and 873 K.

For 773 K, initial droplet diameter: 0.905 mm, camera speed: 20 fps, ambient temperatures measured during evaporation: 772 - 780 K. For 823 K, initial droplet diameter: 0.874 mm, camera speed: 20 fps, ambient temperatures measured during evaporation: 822 - 831 K. For 873 K, initial droplet diameter: 0.816 mm, camera speed: 20 fps, ambient temperatures measured during evaporation: 873 - 882 K.

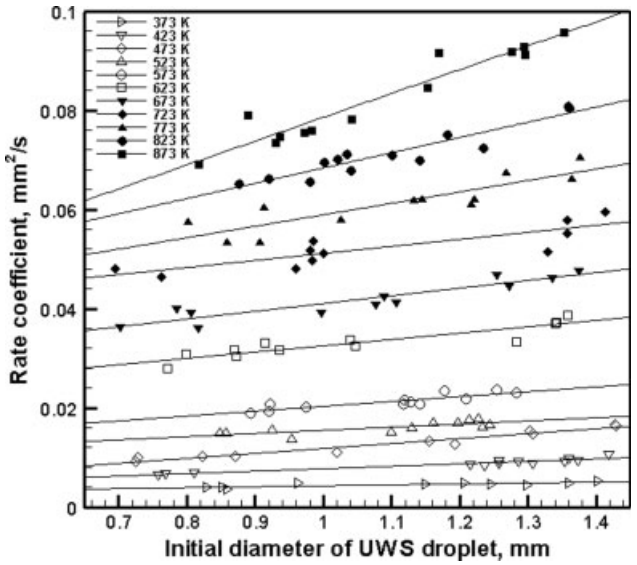

Figure 14. Rate coefficients of the first evaporation stage for various initial diameters of UWS droplets and ambient temperatures.

For ambient temperatures of 773, 823, and 873 K

Figure 13 presents normalized evaporation histories of UWS droplets at 773–873 K. In this temperature range, the second-stage diminishment rate becomes faster than the first-stage rate. This is primarily because droplet microexplosion occurs more aggressively when compared with the case of 673 and 723 K; Figures 13 reveals more intense second-

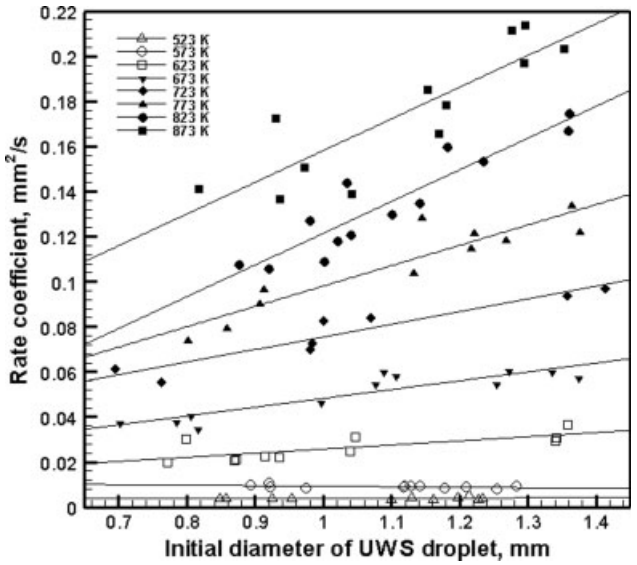

Figure 15. Rate coefficients of the second evaporation stage for various initial diameters of UWS droplets and ambient temperatures.

stage evaporation behaviors than Figure 11. Note that the difference in diminishment rates of both the first and the second stages becomes larger as ambient temperature rises from 773 to 873 K.

In this experiment, solidified deposits were still observed to remain up to 773 K, while almost no deposit was found for ambient temperatures of 823 and 873 K. It is known that ammelide is completely eliminated at about 873 K, while ammeline requires temperatures over 973 K.[7] Therefore, it can be deduced that quite a tiny amount of ammeline is produced during the evaporation of UWS droplet. If ammeline was produced considerably, then a certain amount of deposit would be observed even at temperatures exceeding 823 K. Also, it is known that CYA is completely disappeared below 673 K.[7] As a consequence, the deposits remaining at temperatures from 673 to 773 K are mainly composed of ammelide.

Initial diameter effect on the evaporation of UWS droplet

Figures 14 and 15, respectively, present the first- and second-stage diminishment rate coefficients of UWS droplets evaporating at temperatures from 373 to 873 K (by rising 50 K) with a variety of initial droplet diameters. It should be noted that the range of ambient temperature measured during evaporation is somewhat different data by data. Averaged lower and upper bounds and their standard deviations (presented in parenthesis) are as follows; for 373 K: 370.1 K (1.6 K)–374.2 K (1.6 K), for 423 K: 420.7 K (1.8 K)–425.5 K (1.9 K), for 473 K: 469.8 K (1.3 K)–475.8 K (2.3 K), for 523 K: 517.8 K (2.0 K)–526.4 K (1.6 K), for 573 K: 568.6 K (1.1 K)–579.0 K (1.3 K), for 623 K: 620.6 K (1.0 K)–627.5 K (2.0 K), for 673 K: 671.2 K (1.3 K)–678.0 K (1.1 K), for 723 K: 721.4 K (1.3 K)–729.9 K (1.7 K), for 773 K: 770.7 K (0.8 K)–779.0 K (1.7 K), for 823 K: 819.8 K (0.9 K)–829.8 K (1.1 K), for 873 K: 870.4 K (0.9 K)–879.0 K (2.1 K).

Also, as shown in Figures 14 and 15, both rate coefficients increase with initial droplet diameter for all temperatures except the second-stage evaporation at 573 K. In addition, the least square fits indicate that the increment of each coefficient with initial droplet diameter becomes larger as ambient temperature increases.

Conclusions

In this study, the evaporation behavior of UWS droplet was investigated using suspended droplet experiment. Through a number of repeated measurements, evaporation rates were extracted for a variety of initial droplet diameters and ambient temperatures. As a consequence, the current study helps to understand the evaporation characteristic of UWS droplet quantitatively as well as qualitatively. Furthermore, this study provides some empirical data required in modeling or simulation works on urea-SCR system. A summary of the results is as follows.

(1) On the basis of the current observations, the evaporation behavior of UWS droplet can be categorized into several groups according to ambient temperature. At 373 and 423 K, UWS droplet evaporates without being divided into two stages. At 473 and 523 K, both evaporation periods of the first and second stages commonly show linear diminishment, while they are obviously distinguished by the difference in their rates. At 573 and 623 K, weak microexplosion appears and the first-stage rate exceeds the second-stage rate. At 673 and 723 K, strong microexplosion appears and the first-stage rate almost equals the second-stage rate. At 773 to 873 K, very strong microexplosion appears and second-stage rate exceeds the first-stage rate.

(2) After the complete depletion of liquid component constituting UWS droplet, solidified deposit is observed to remain at temperatures below 773 K and its amount is reduced with increase in ambient temperature, while there is almost no deposit remained at temperatures above 823 K.

(3) Both diminishment rates of the first and second evaporation stages increase as the initial size of UWS droplet increases. Also, the increment of each rate coefficient with initial droplet size becomes larger as ambient temperature increases.

Acknowledgments

This study was supported by the CEFV (Center for Environmentally Friendly Vehicle) of Eco-STAR project from MOE (Ministry of Environment, Republic of Korea). Special thanks are also indebted to Dr. Q. S. Khan who gave a hand in the preparation of this experiment.

Literature Cited

1. http://www.DieselNet.com, Selective Catalytic Reduction. In: DieselNet Technology Guide, 2002.
2. Koebel M, Elsener M. Determination of urea and its thermal decomposition products by high-performance liquid chromatography. *J Chromatogr A*. 1995;689:164–169.
3. Yim SD, Kim SJ, Baik JH, Nam IS, Mok YS, Lee JH, Cho BK, Oh SH. Decomposition of urea into NH_3 for the SCR process. *Ind Eng Chem Res*. 2004;43:4856–4863.
4. Kleemann M, Elsener M, Koebel M, Wokaun A. Hydrolysis of isocyanic acid on SCR catalysts. *Ind Eng Chem Res*. 2000;39:4120–4126.
5. Koebel M, Elsener M, Kleemann M. Urea-SCR: a promising technique to reduce NO_x emissions from automotive diesel engines. *Catal Today*. 2000;59:335–345.
6. Koebel M, Elsener M, Marti T. NO_x-reduction in diesel exhaust gas with urea and selective catalytic reduction. *Combust Sci Tech*. 1996;121:85–102.
7. Schaber PM, Colson J, Higgins S, Thielen D, Anspach B, Brauer J. Thermal decomposition (pyrolysis) of urea in an open reaction vessel. *Thermochim Acta*. 2004;424:131–142.
8. Fang HL, DaCosta HFM. Urea thermolysis and NO_x reduction with and without SCR catalysts. *Appl Catal B: Environ*. 2003;46:17–34.
9. Koebel M, Elsener M, Madia G. Reaction pathways in the selective catalytic reduction process with NO and NO_2 at low temperatures. *Ind Eng Chem Res*. 2001;40:52–59.
10. Seker E, Yasyerli N, Gulari E, Lambert C, Hammerle RH. NO_x reduction by urea under lean conditions over single step sol-gel Pt/alumina catalyst. *Appl Catal B: Environ*. 2002;37:27–35.
11. Sullivan JA, Doherty JA. NH_3 and urea in the selective catalytic reduction of NO_x over oxide-supported copper catalysts. *Appl Catal B: Environ*. 2005;55:185–194.
12. Birkhold F, Meingast U, Wassermann P, Deutschmann O. Modeling and simulation of the injection of urea-water-solution for automotive SCR $DeNO_x$-systems. *Appl Catal B: Environ*. 2007;70:119–127.
13. Faeth GM. Evaporation and combustion of sprays. *Prog Energy Combust Sci*. 1983;9:1–76.
14. Sirignano WA. Fuel droplet vaporization and spray combustion theory. *Prog Energy Combust Sci*. 1983;9:291–322.
15. Law CK. Internal boiling and superheating in vaporizing multicomponent droplets. *AIChE J*. 1978;24:626–632.

16. Avedisian CT, Glassman I. High pressure homogeneous nucleation of bubbles within superheated binary liquid mixtures[1]. *J Heat Transfer*. 1981;103:272–280.
17. Shepherd JE, Sturtevant B. Rapid evaporation at the superheat limit. *J Fluid Mech*. 1982;121:379–402.
18. Wang CH, Liu XQ, Law CK. Combustion and microexplosion of freely falling multicomponent droplets. *Combust Flame*. 1984;56: 175–197.
19. Lara-Urbaneja P, Sirignano WA. Theory of transient multicomponent droplet vaporization in a convective field, *18th Symposium (Int'l) on Combustion*, The Combustion Institute, Pittsburgh, PA, 1981:1365–1374.
20. Chiu HH. Advances and challenges in droplet and spray combustion. I. Toward a unified theory of droplet aerothermochemistry. *Prog Energy Combust Sci*. 2000;26:381–416.
21. Law CK. Recent advances in droplet vaporization and combustion. *Prog Energy Combust Sci*. 1982;8:171–201.
22. Law CK, Prakash S, Sirignano WA. Theory of convective, transient, multicomponent droplet vaporization, *16th Symposium (Int'l) on Combustion,* The Combustion Institute, Pittsburgh, PA, 1977:605–617.
23. Ghassemi H, Baek SW, Khan QS. Experimental study on binary droplet evaporation at elevated pressures and temperatures. *Combust Sci Tech*. 2006;178:1031–1053.
24. Ghassemi H, Baek SW, Khan QS. Experimental study on evaporation of kerosene droplets at elevated pressures and temperatures. *Combust Sci Tech*. 2006;178:1669–1684.
25. http://webbook.nist.gov/chemistry/,NIST Chemistry WebBook, NIST Standard Reference Database No. 69, 2005.
26. Musa SNA, Saito M, Furuhata T, Arai M. Evaporation characteristics of a single aqueous urea solution droplet. ICLASS-2006, Kyoto, Paper ID ICLASS06-195, 2006.

Manuscript received July 18, 2008, and revision received Apr. , 2009.